Vortex structure transformation of $BaTiO_3$ nanoparticles through the gradient function

L. Hong,[1] A. K. Soh,[1,a)] S. Y. Liu,[1] and L. Lu[2]
[1]*Department of Mechanical Engineering, The University of Hong Kong, Hong Kong, China*
[2]*Department of Mechanical Engineering, National University of Singapore, 9 Engineering Drive 1, Singapore 117576, Singapore*

(Received 29 April 2009; accepted 27 June 2009; published online 31 July 2009)

Phase field method has been used to simulate the vortex structures in $BaTiO_3$ (BTO) nanoparticles. Through the modulation of the gradient coefficients, vortices are found to transform in a path of monoclinic $M_A \rightarrow$ orthorhombic $\rightarrow$ monoclinic $M_C \rightarrow$ tetragonal. Although the gradient coefficients vary significantly, the change in gradient energy is remarkably small. The simulation results show that the rotation and magnitude reduction in polarization dipoles increase the bulk energy, which induces the vortex transformation process in BTO nanoparticles. Moreover, the existence of monoclinic phase is a necessity to start the polarization rotation as well as the vortex transformation process. © *2009 American Institute of Physics*. [DOI: 10.1063/1.3186038]

I. INTRODUCTION

Vortex structure (VS) is the identity of zero-dimensional ferroelectric nanoparticles under open-circuit condition. first-principles-based and phase field simulations have shown that the $BaTiO_3$ (BTO) nanoparticle has a rhombohedral VS (Ref. 1) pointing along $\langle 111 \rangle$ while the $\langle 001 \rangle$ is the direction of the tetragonal VS of the $PbZr_{1-x}Ti_xO_3$ (Ref. 2) and $PbTiO_3$ (PTO)[3,4] nanoparticles. Note that the tetragonal VS is defined as one with its vortex direction pointing along the tetragonal direction; and the other types of VSs, i.e., orthorhombic, monoclinic, and rhombohedral, are also defined in a similar manner. A question to be addressed is whether these VSs could transform in a single ferroelectric nanoparticle, just like spontaneous polarizations do in ferroelectrics.

Domain wall energy is an important part of the internal energies as there are always domain walls between different domains in a ferroelectric. The contribution of the domain wall energy to the total energy can be modified through the introduction of defects, which always have pinning interactions with the domain walls,[5,6] e.g., oxygen vacancy defects tend to aggregate around 90° domain walls.[7,8] Attempts will be made in the present study to relate the transformations of the VSs (monoclinic, orthorhombic, and tetragonal states) to the variations of the coefficients of the domain wall energy at room temperature. In the present study, there are two possible monoclinic VSs, which are designated as M_A and M_C for vortex direction along $[xzz]$ and $[0yz]$, respectively. Note that similar definitions were adopted for the directions of polarization dipoles.[9] Moreover, the focus of the present study is on BTO nanoparticle and its vortex transformation, which is different from that of our previous paper,[4] in which the influence of size-dependent electrostatic energy on the ferroelectric nanodot domain structure was studied. Due to the small size of the VS and the simulation model devised, there are no well defined domain regions with homogeneous polarization directions and, thus, no distinguishable domain wall areas. Therefore, the term "domain wall energy" is replaced with "gradient energy" in the following text to represent the energy contribution from all the transitional polarization dipoles. However, the approach to influence the gradient energy is in principle the same as that to affect the domain wall energy in ferroelectrics.

II. PHASE FIELD MODEL

In the present study, the phase field method is employed to devise a three-dimensional BTO nanoparticle model under open-circuit condition, where the ferroelectric core part is embedded in a nonpolarization medium to represent an individual nanostructure. Note that similar approaches have been adopted by Wang *et al.*[3] and Slutsker *et al.*[10] The open-circuit condition is required to minimize the unscreening electrostatic field through the formation of vortex domain structures in confined ferroelectric nanostructures.[11] Moreover, the domain structures of ferroelectric nanoarrays under such condition have been observed recently through the use of piezoresponse force microscopy,[12] which provides a direct comparison of theoretical and experimental results. The equilibrium condition of the present model is achieved by minimizing the total free energy $F=F_{GL}+F_{electro}+F_{ela}$, where F_{GL}, $F_{electro}$, and F_{ela} are Ginzburg–Landau (GL) potential, the energy of electrostatic interactions, and the elastic energy of the system, respectively.

The GL potential is given by $F_{GL}=\int_V [f_L(P_i)+f_G(P_{i,j})]dV$, which includes an eighth-order polynomial $f_L(P_i)$ for the Landau–Devonshire potential as the bulk energy, and a gradient function to depict the domain wall and interface energies, where P_i represent spontaneous polarizations. For the three-dimensional polarization matrix, $i,j=1,2,3$, $f_L(P_i)$ is defined as follows:

a)Author to whom correspondence should be addressed. Electronic mail: aksoh@hkucc.hku.hk. Tel.: +852-28598061. FAX: +852-28585415.

$$f_L(P_i) = \alpha_1(P_1^2 + P_2^2 + P_3^2) + \alpha_{11}(P_1^4 + P_2^4 + P_3^4) + \alpha_{12}(P_1^2P_2^2 + P_2^2P_3^2 + P_3^2P_1^2) + \alpha_{111}(P_1^6 + P_2^6 + P_3^6) + \alpha_{112}[P_1^4(P_2^2 + P_3^2) + P_2^4(P_1^2 + P_3^2) + P_3^4(P_1^2 + P_2^2)] + \alpha_{123}(P_1^2P_2^2P_3^2) + \alpha_{1111}(P_1^8 + P_2^8 + P_3^8) + \alpha_{1122}(P_1^4P_2^4 + P_2^4P_3^4 + P_3^4P_1^4) + \alpha_{1112}[P_1^6(P_2^2 + P_3^2) + P_2^6(P_1^2 + P_3^2) + P_3^6(P_1^2 + P_2^2)] + \alpha_{1123}(P_1^4P_2^2P_3^2 + P_2^4P_3^2P_1^2 + P_3^4P_1^2P_2^2), \quad (1)$$

where α_1 is a temperature-dependent coefficient, and the others are assumed to be temperature independent. The inclusion of eighth-order constants in Landau–Devonshire potential has helped to reproduce the bulk properties including the dielectric and piezoelectric constants, as well as the phase transition temperatures and the monoclinic phase.[9,13] The gradient term in the GL potential is described as

$$f_G(P_{i,j}) = \tfrac{1}{2}G_{11}(P_{1,1}^2 + P_{2,2}^2 + P_{3,3}^2) + G_{12}(P_{1,1}P_{2,2} + P_{2,2}P_{3,3} + P_{3,3}P_{1,1}) + \tfrac{1}{2}G_{44}[(P_{1,2} + P_{2,1})^2 + (P_{2,3} + P_{3,2})^2 + (P_{1,3} + P_{3,1})^2] + \tfrac{1}{2}G'_{44}[(P_{1,2} - P_{2,1})^2 + (P_{2,3} - P_{3,2})^2 + (P_{1,3} - P_{3,1})^2], \quad (2)$$

where G_{11}, G_{12}, G_{44}, and G'_{44} are the gradient energy coefficients and the commas in the subscripts denote spatial differentiation.

The energy of electrostatic interactions induced by inhomogeneous polarizations inside the ferroelectric nanoparticle is given by $F_{\text{electro}} = -\frac{1}{2}\int_V E_i P_i dV$, where E_i represents the electrostatic field, which is the negative gradient of the electrostatic potential ϕ obtained from Maxwell's equation. The elastic energy is calculated using $F_{\text{ela}} = \frac{1}{2}\int_V c_{ijkl}(\varepsilon_{ij} - \varepsilon_{ij}^0)(\varepsilon_{kl} - \varepsilon_{kl}^0)dV$, in which c_{ijkl} and ε_{ij} are the elastic stiffness tensors and total strains, respectively. The spontaneous strains $\varepsilon_{ij}^0 = Q_{ijkl}P_kP_l$ are generated during the transformation of crystal structures, and Q_{ijkl} are the electrostrictive coefficients.

The final equilibrium state of the spontaneous polarizations can be determined by solving the time-dependent GL equation given by

$$\frac{\partial P_i(\mathbf{r},t)}{\partial t} = -L\frac{\delta F}{\delta P_i(\mathbf{r},t)}, \quad (3)$$

where $\mathbf{r}$ denotes spatial vector. In addition, t and L are the time and kinetic coefficient, respectively.

III. RESULTS AND DISCUSSION

A. Simulation parameters

The three-dimensional BTO nanoparticle model is composed of $48 \times 48 \times 48$ discrete grids, in which the core part $16 \times 16 \times 16$ is ferroelectric and the outer part is a nonpolarization medium. The details have been elaborated in our paper[4] and, therefore, will not be reiterated here. The BTO parameters employed are listed in Ref. 14. Since insufficient experimental results are available to characterize the exact gradient coefficients, isotropic constants taken from different simulation models of BTO nanostructures[17,18] are adopted in the present study. The value of the dimensionless gradient coefficient G_{11}^* is set from 1.2 to 4.2 $\left(G_{12}^*=0,\ G_{44}^*=G_{44}'^*=\frac{1}{2}G_{11}^*\right)$ to demonstrate the influence of the gradient function on the VS. The basis for selection of G_{11}^* values is explained below. If the grid spacing $\Delta x = l_0$ is set as 1 nm, the reference value of the gradient energy coefficient is $G_{110} = l_0^2|\alpha_{1,T=27\,^\circ\text{C}}| = 3.6 \times 10^{-11}$ $\text{C}^{-2}\,\text{m}^4\,\text{N}$. Since $G_{44} = 2.0 \times 10^{-11}$ $\text{C}^{-2}\,\text{m}^4\,\text{N}$ is deemed a reliable value,[19] $G_{44}^* = G_{44}/G_{110} = 0.6$ and, therefore, the starting value of the dimensionless gradient coefficient is calculated as $G_{11}^* = 1.2$. Note that the material is supposed to be defect-free at the said starting value. Thus, it is perfectly reasonable to assume that the gradient coefficient increases with the increase in defects. It is worth noting that if G_{11}^* is assumed to be significantly larger than 4.2, the domain structures of the BTO nanoparticles become unstable. The relative dielectric permittivity of the BTO nanoparticle is assumed to be 200.

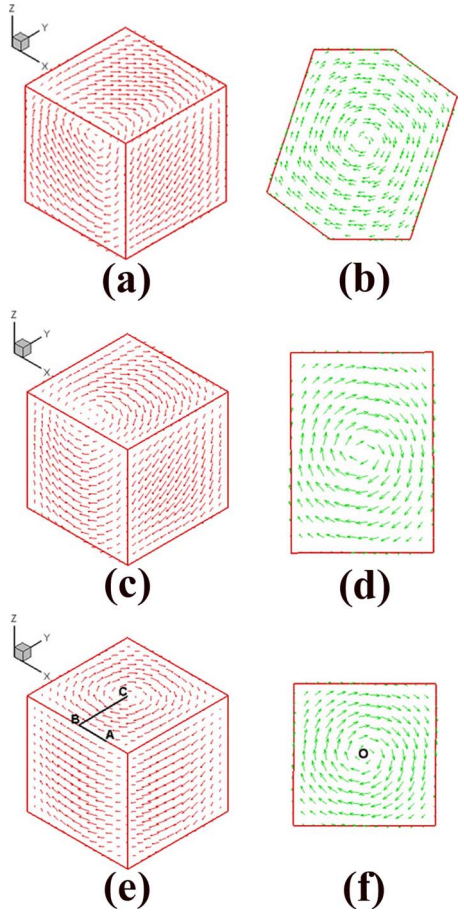

FIG. 1. (Color online) Monoclinic M_A, orthorhombic, and tetragonal VSs of BTO nanoparticles at room temperature for gradient coefficients G_{11}^* of 1.2 [(a) and (b)], 2.4 [(c) and (d)], and 3.6 [(e) and (f)], respectively. (a), (c), and (e) show the three-dimensional vortex patterns; (b), (d), and (f) illustrate the $(\bar{1}2\bar{2})$, $(01\bar{1})$, and $(00\bar{1})$ vortex planes traversing the central spot of the corresponding VS. A, B, and C in (e) indicate the three monoclinic M_A, orthorhombic, and tetragonal vortex centers on the top surface of the respective VS, and O in (f) is the volume central of the nanoparticle.

B. Different VSs

Figure 1 presents the creation of the monoclinic, orthorhombic, and tetragonal VSs by the adoption of different

gradient coefficients in a single BTO nanoparticle under room temperature. Note that all these equilibrium processes are evolved from initial random noises. In addition, the plane vertical to the vortex direction possesses the main feature of the VS. When G_{11}^* is equal to 1.2, the monoclinic M_A VS is produced [Fig. 1(a)], which is composed of orthorhombic and monoclinic polarization dipoles [Fig. 1(b)], where most of the dipoles are parallel with the vortex boundaries on the exterior surfaces of the nanoparticle. This characteristic of dipole alignment is also exhibited by other VSs due to the adoption of open-circuit condition. Note that the rhombohedral VS of the BTO nanoparticle, which has been discovered by first-principles-based calculations,[1] has not been found in the proposed model. This is likely due to implementations of zero interface polarizations as well as periodic boundary conditions on the outer surfaces of the present model.[3,10] However, the lack of evidence for the existence of rhombohedral VS in the proposed model does not affect the phenomena and mechanism observed in the present study. Figures 1(c) and 1(d) depict the orthorhombic VS when G_{11}^* is increased to 2.4. There are two distinctive features that differentiate the orthorhombic VS from the monoclinic M_A, i.e., (i) coexistence of the orthorhombic and tetragonal polarization dipoles, and (ii) the 90° dipole regions with more significant gradient energy separate the orthorhombic VS into four parts. With the increase in gradient coefficient, the orthorhombic VS is transformed into monoclinic M_C, and eventually to tetragonal VS. The tetragonal dipoles and 90° dipole regions with more significant gradient energy constitute the major part of the structure illustrated in Figs. 1(e) and 1(f). Note that this is the first time that the tetragonal VS is found in a BTO nanostructure, which indicates that besides the rhombohedral VS whose direction conforms to the polarization direction at the ground state of BTO, other asymmetric VSs could also be realized through the control of gradient function. Moreover, one interesting phenomenon is that the VSs change a little when the temperature is decreased to 10 K from room temperature, which has also been illustrated by first-principles-based calculations.[20]

C. Vortex transformation path

To characterize these unique VSs of ferroelectric nanoparticles, the toroidal moment of polarization $\mathbf{G}=(2N)^{-1}\Sigma_i \mathbf{R}_i \times \mathbf{p}_i$ and the total net polarization $\mathbf{P}=N^{-1}\Sigma_i \mathbf{p}_i$ are adopted,[2] where $\mathbf{p}_i$ is the polarization dipole of node i located at $\mathbf{R}_i$ and N is the number of ferroelectric nodes in the present model. Note that $\mathbf{P}$ is null regardless of the type of VSs considered and, therefore, it is not suitable for differentiating between VSs. Due to the minimization of electrostatic energy and the adoption of open-circuit condition, VS should always be a stable one in a confined nanoparticle. Therefore, it is not difficult to interpret the appearance of the four different VSs in this study. The VS transformation in a BTO nanoparticle is actually the rotation process of vortex direction; however, the position of vortex center is kept unchanged at the central point of the nanoparticle. The transformation path of the vortices in a BTO nanoparticle can be summarized as $AO \rightarrow BO \rightarrow CO$ (Fig. 1) or monoclinic M_A $\rightarrow$ orthorhombic $\rightarrow$ monoclinic $M_C \rightarrow$ tetragonal vortex (Fig. 2), with the increase in gradient coefficient G_{11}^*. The ratio between the three toroidal moment components, G_x, G_y, and G_z, determines the vortex direction and, thus, classifies the VSs into different categories. Note that approximate ratios, and not ratios between integers of G_x, G_y, and G_z, are adopted to mark the VS transformation path. When G_{11}^* is equal to 1.2, the direction of the VS in Fig. 1(a) is calculated to be approximately $[\bar{1}2\bar{2}]$ from the ratio of $G_x:G_y:G_z$ given in Fig. 2; therefore, it falls into the category of monoclinic M_A VS. It can be clearly seen from Fig. 2 that the direction of the monoclinic M_A VS continuously rotates on the (011) plane until the appearance of orthorhombic VS when G_{11}^* reaches 2.2, where the absolute ratio value of $G_y:G_z$ is close to 1 and G_x is approximately 0. However, the latter structure only appears in a short range of G_{11}^* (i.e., from 2.2 to 2.4) due to the rapid decrease in G_y, which induces the formation of monoclinic M_C VS. With the increase in gradient coefficient, the monoclinic M_C VS starts to rotate on the (100) plane, and finally when G_{11}^* approaches 3.0 the tetragonal VS becomes stable with near vanishment of G_x and G_y.

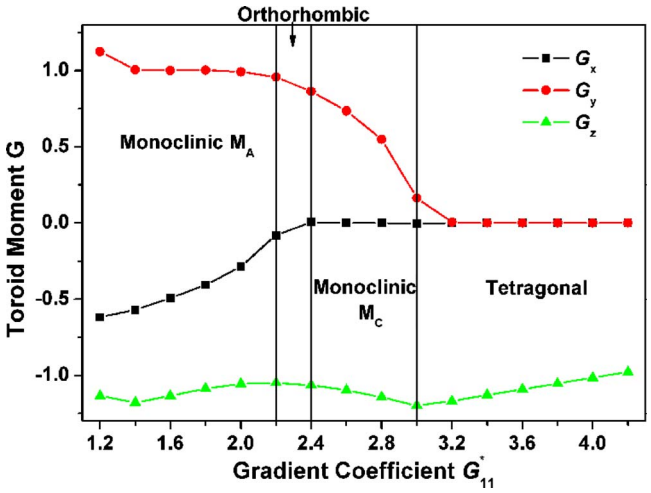

FIG. 2. (Color online) Plot of toroidal moment of polarization vs G_{11}^* for BTO nanoparticles under room temperature.

D. The intrinsic mechanism

In order to understand the intrinsic mechanism in the transformation process, the variations of the dimensionless energies with respect to G_{11}^* are plotted in Fig. 3. Since vortex exists in the whole transformation, the electrostatic energy is minimized to close to zero for all VSs (as shown in Fig. 3). The change in gradient energy is remarkably small compared with the variation of the gradient coefficients due to the competitive increase in the bulk energy, which arises from the rotation as well as magnitude reduction in polarization dipoles. The obvious increase in bulk energy in Fig. 3 dominates the change in the total energy throughout this nanoparticle's transformation process. With references to Figs. 2 and 3, the monoclinic and orthorhombic dipoles change to tetragonal ones gradually by increasing the gradient coefficient, leading to the increase in the bulk energy; whereas, the variation of gradient coefficient leads to a rela-

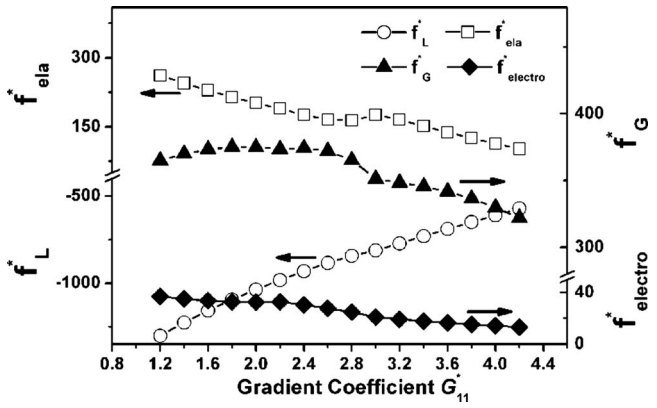

FIG. 3. Variations of dimensionless bulk energy density f^*_L, gradient energy density f^*_G, electrostatic energy density $f^*_{electro}$, and elastic energy density f^*_{ela} with respect to the dimensionless gradient coefficient G^*_{11} of BTO nanoparticles.

tively small change in the gradient energy. Before the end of the monoclinic M_C VS, the rotation of polarization dipoles makes the major contribution to the increase in bulk energy, whereas, the gradient energy remains constant. By increasing the gradient coefficient after the tetragonal VS has commenced, the gradient energy begins to decrease gradually due to the decrease in magnitude of the dipoles, especially those in the vicinity of the dipole regions with more significant gradient energy. Note that such dipole regions do not change significantly as there is only one vortex in any stable VS, which is unlike the case given in Ref. 21. Moreover, the majority of the gradient energy is located around the vortex center. The larger the gradient coefficient G^*_{11} is, the smaller is the bulk energy in magnitude, and the lesser is the averaged magnitude of polarization dipoles. Note that the change in elastic energy, which is not significant compared with the variation of the bulk energy, is also induced by the variation of polarization dipoles during the VS transformation.

Last but not the least, in order to validate the vortex transformation process, two additional simulation cases are carried out. In the first case, the range of gradient coefficients employed in the above study is used to investigate the PTO nanoparticle devised in our previous paper.[4] The results indicate that only tetragonal VSs appear as the stable ferroelectric domain structure in PTO nanoparticles. This is because there is only a single ferroelectric phase transition from cubic to tetragonal in bulk PTO. The second simulation case is a new BTO nanoparticle model in which a sixth-order polynomial[15] is employed as the bulk energy. No clear VS transformation is found in this BTO nanoparticle model. This is probably due to the fact that the sixth-order bulk energy cannot support a monoclinic phase in BTO.[9] Therefore the formation of monoclinic phase is required to induce the present vortex transformation process of the BTO nanoparticles.

IV. SUMMARY

Interface pinning interaction in ferroelectric crystals is known to influence the domain wall properties[6,22–24] and, therefore, would probably affect the gradient coefficients. Moreover, with the decrease in the functional size to nanoscale, the volume ratio of the dipole regions with more significant gradient energy, e.g., domain wall, will be greatly increased. Therefore, the variation of gradient coefficients would significantly affect the properties and behavior of ferroelectric nanoparticles. However, the gradient energy does not vary significantly as expected with the variation of gradient coefficients. This small variation in gradient energy is insignificant compared with the increase in bulk energy due to the rotation and magnitude reduction in polarization dipoles, which induces the vortex transformation process in BTO nanoparticles. In addition, the existence of a monoclinic phase of the starting VS constitutes the necessary condition to intrigue the rotation process of polarization dipoles, and thus the vortex transformation path. The discovery of vortex transformation in BTO nanoparticles may have an important impact on the potential applications of zero-dimensional ferroelectric materials in terms of modulating VS through external control.

ACKNOWLEDGMENTS

Support from the Research Grants Council of the Hong Kong Special Administrative Region, China (Project Nos. HKU716007E and 716508E) is acknowledged. The authors gratefully acknowledge the support of the Computer Center of The University of Hong Kong.

[1]H. Fu and L. Bellaiche, Phys. Rev. Lett. **91**, 257601 (2003).
[2]I. Naumov, L. Bellaiche, and H. Fu, Nature (London) **432**, 737 (2004).
[3]J. Wang, M. Kamlah, T. Y. Zhang, Y. L. Li, and L. Q. Chen, Appl. Phys. Lett. **92**, 162905 (2008).
[4]L. Hong, A. K. Soh, S. Y. Liu, and L. Lu, J. Phys. D **42**, 122005 (2009).
[5]J. F. Scott and M. Dawber, Appl. Phys. Lett. **76**, 3801 (2000).
[6]A. Agronin, Y. Rosenwaks, and G. Rosenman, Appl. Phys. Lett. **88**, 072911 (2006).
[7]Y. Xiao, V. B. Shenoy, and K. Bhattacharys, Phys. Rev. Lett. **95**, 247603 (2005).
[8]L. Hong, A. K. Soh, Q. G. Du, and J. Y. Li, Phys. Rev. B **77**, 094104 (2008).
[9]D. Vanderbilt and M. H. Cohen, Phys. Rev. B **63**, 094108 (2001).
[10]J. Slutsker, A. Artemev, and A. Roytburd, Phys. Rev. Lett. **100**, 087602 (2008).
[11]I. Ponomareva, I. I. Naumov, and L. Bellaiche, Phys. Rev. B **72**, 214118 (2005).
[12]B. J. Rodriguez, X. S. Gao, L. F. Liu, W. Lee, I. I. Naumov, A. M. Bratkovsky, D. Hesse, and M. Alexe, Nano Lett. **9**, 1127 (2009).
[13]Y. L. Li, L. E. Cross, and L. Q. Chen, J. Appl. Phys. **98**, 064101 (2005).
[14]The parameters are from Refs. 13, 15, and 16: $\alpha_1=4.124\times10^5(T-115)$, $\alpha_{11}=-2.097\times10^8$, $\alpha_{12}=7.974\times10^8$, $\alpha_{111}=1.294\times10^9$, $\alpha_{112}=-1.950\times10^9$, $\alpha_{123}=-2.500\times10^9$, $\alpha_{1111}=3.863\times10^{10}$, $\alpha_{1112}=2.529\times10^{10}$, $\alpha_{1122}=1.637\times10^{10}$, $\alpha_{1123}=1.367\times10^{10}$, $c_{11}=1.755\times10^{11}$, $c_{12}=8.464\times10^{10}$, $c_{44}=1.082\times10^{11}$, $Q_{11}=0.11$, $Q_{12}=-0.043$, and $Q_{44}=0.059$ (in SI units and T in °C).
[15]N. A. Pertsev, A. G. Zembilgotov, and A. K. Tagantsev, Phys. Rev. Lett. **80**, 1988 (1998).
[16]N. A. Pertsev and H. Kohlstedt, e-print arXiv:cond-mat/0603762v2.
[17]Y. L. Li and L. Q. Chen, Appl. Phys. Lett. **88**, 072905 (2006).
[18]Y. L. Li, S. Y. Hu, D. Tenne, A. Soukiassian, D. G. Schlom, X. X. Xi, K. J. Choi, C. B. Eom, A. Saxena, T. Lookman, Q. X. Jia, and L. Q. Chen, Appl. Phys. Lett. **91**, 112914 (2007).
[19]J. Hlinka and P. Marton, Phys. Rev. B **74**, 104104 (2006).
[20]S. Prosandeev, I. Ponomareva, I. Naumov, I. Kornev, and L. Bellaiche, J. Phys.: Condens. Matter **20**, 193201 (2008).
[21]J. Wang, M. Kamlah, and T. Y. Zhang, J. Appl. Phys. **105**, 014104 (2009).
[22]V. Gopalan, V. Dierolf, and D. A. Scrymgeour, Annu. Rev. Mater. Res. **37**, 449 (2007).
[23]Y. L. Wang, A. K. Tagantsev, D. Damjanovic, and N. Setter, Appl. Phys. Lett. **91**, 062905 (2007).
[24]D. Shilo, H. Drezner, and A. Dorogoy, Phys. Rev. Lett. **100**, 035505 (2008).